NUMERICAL AND EXPERIMENTAL ANALYSES OF THE SOUND ABSORPTION OF PLAIN WEAVE FABRICS

Cai Zenong, Li Xianhui, Gai Xiaoling, Xing Tuo, Zhang Bin and Wang Fang

Beijing Municipal Institute of Labor Protection, Beijing 100054, China
Beijing Key Laboratory of Environment Noise and Vibration, Beijing 100054, China
email: lixianh@vip.sina.com

Well-designed thin lightweight fabrics can effectively replace bulky porous materials traditionally used in sound absorption. In this paper, Johnson-Champoux-Allard (JCA) model is used to analyze the sound absorption characteristics of monofilament plain weave fabrics. Detailed 3D geometric models are built for a set of plain weave samples. The parameters required by the JCA model, such as geometric tortuosity, flow resistivity, and porosity, are obtained numerically from finite element analysis. It is observed that the crimp heights have significant influence on the flow resistivity and porosity, which determine the sound absorption characteristics of the plain weave fabrics. Experimental results from the impedance tube test agree well with the numerical predictions. By improving the weaving machine and choosing appropriate diameter of monofilament, an acoustic textile can be fabricated for the engineering application.
Keywords: sound-absorbing textile, plain weave fabrics, noise absorption

1. Introduction

Textile curtains have been widely used to absorb sound for many years. Because of the flexibility in changing their configuration, people can adjust the reverberation time easier than other approaches. Generally, textile curtains need enough thickness and surface mass density to have good sound absorption performance. However, thin, light textile curtains are much cheaper and provide a promising alternative. Recently, Pieren [1] presented a theoretical model to predict the absorption coefficient of a thin woven fabric backed by a cavity. The fabric is represented by an air flow resistance and its surface mass density. An acoustic inverse method is employed to obtain the air flow resistance. Later, Pieren et.al [2] proposed a more elaborate model considering the intrayarn airflow. Ruiz et.al [3] developed a hybrid model describing the acoustic properties of macroperforated plates backed by woven meshes, where the woven meshes is analysed by a simplified geometric model.

In this paper, we focus on the monofilament plain weave textile. Detailed three-dimensional (3D) geometric models are built for a set of plain weave samples. The effects on the sound absorption of the major parameters of the fabric, such as geometric tortuosity, flow resistivity, and porosity, are investigated. It is observed that the crimp heights have significant influence on the flow resistivity and porosity, which determine the sound absorption characteristics of the plain weave fabrics. Experimental results from the impedance tube test validate the numerical predictions.

2. Model

Based on the microstructure of the plain weave, a 3D geometric mode is built. The FEM method is applied to obtain the parameters which are required in the Johnson-Champoux-Allard model. The JCA model is utilized to predict the absorption coefficients of 3D models.

2.1 Geometry model

Based on following assumptions, the simplified 3D model of plain weave is built:

- In a certain textile, the shape of cross sections of all of threads is circle with the same size of radii.
- The lengthwise sections of the textile are on the basis of the F. T. Peirce model [4] (shown in Fig. 1).
- The threads in the structure are considered as uniform distributed.
- There are small air gaps between the two overlapped threads in order to avoid mistakes in FEM method.

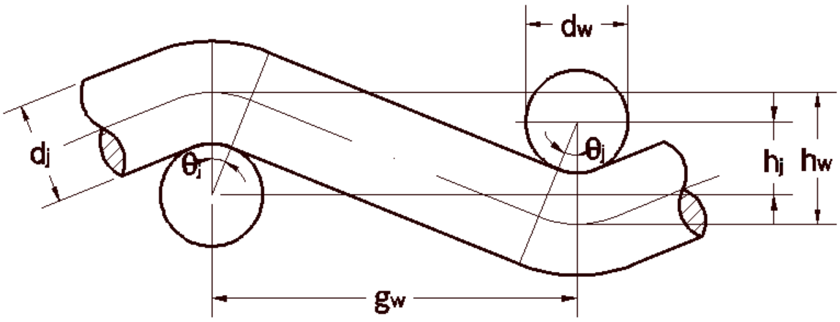

Figure 1: The F. T. Peirce model. (d_j, d_w: diameter of thread, g_w: thread spacing, h_j, h_w: maximum displacement of thread axis normal to the plane of cloth (crimp height), θ_j: weave angle in radians

In fact, in this article, the influence of different crimp heights is considered. Two extreme cases are chosen: 1) $h_j = 0$ (or $h_w = 0$), 2) $h_j = h_w$ as depict in Fig. 2 (a) and Fig. 2 (b), respectively:

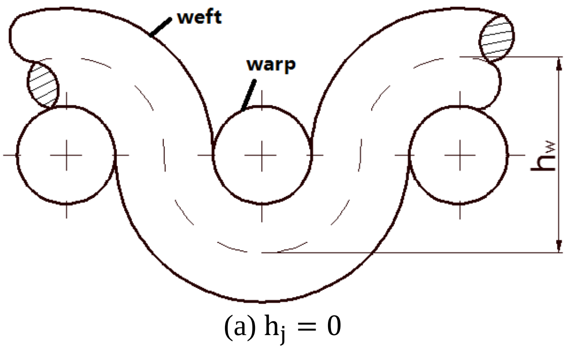

(a) $h_j = 0$

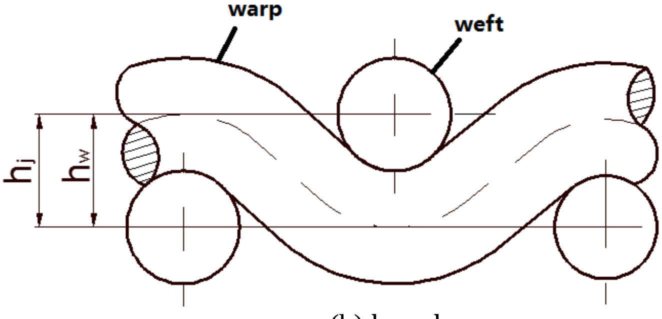

(b) $h_j = h_w$

Figure 2: Two extreme cases of different crimp heights

The 3D models are built shown in Fig. 3:

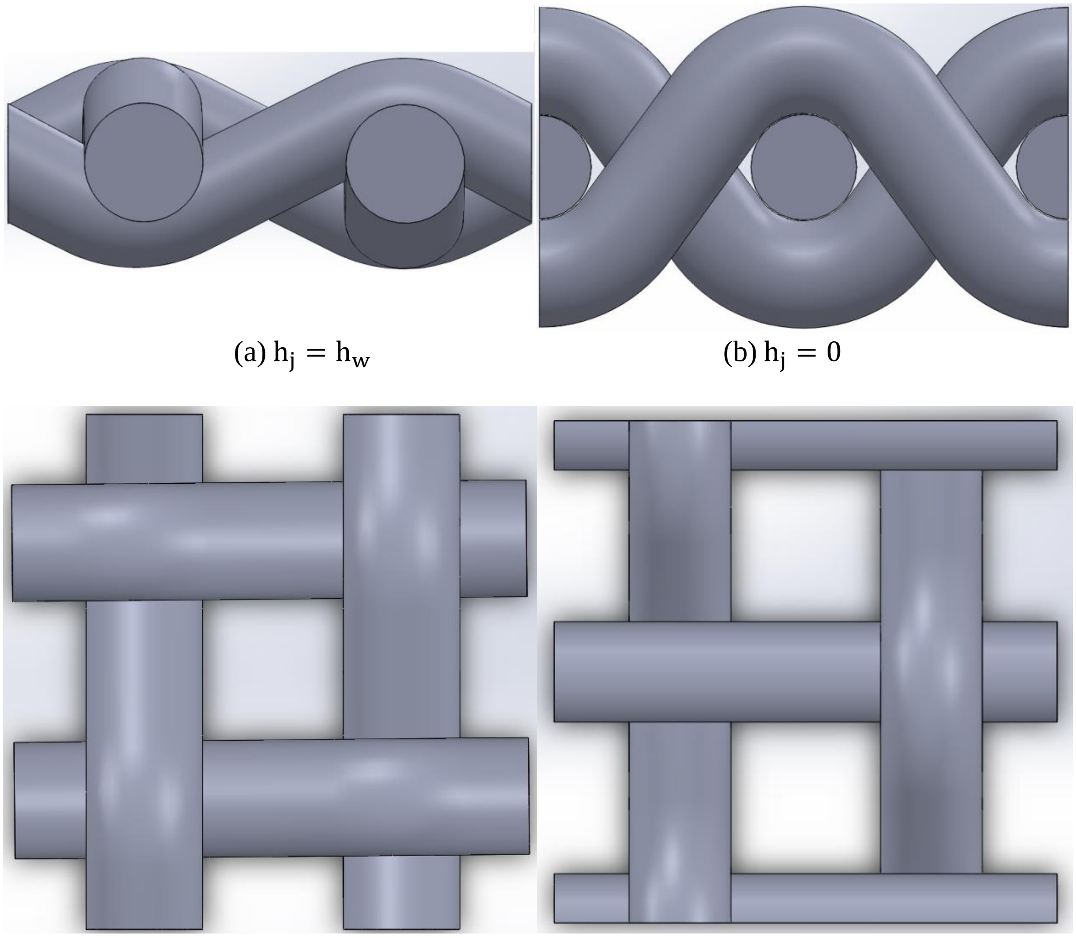

(a) $\mathrm{h_j} = \mathrm{h_w}$ (b) $\mathrm{h_j} = 0$

(c) $\mathrm{h_j} = \mathrm{h_w}$ (d) $\mathrm{h_j} = 0$

Figure 3: 3D models

The diameters of monofilaments and the monofilament spacing of the 3D model are consistent with the samples we use in experimental methods, and the details will be mentioned in the Section 2.3.

2.2 Johnson-Champoux-Allard model

In this article, the FEM method is used to calculate the intrinsic parameters in our 3D models, and these characteristics are substituted into the JCA model to derive the normal absorption coefficients.

The effective density in the JCA model [5] [6] is given by

$$\tilde{\rho}(\omega) = \frac{\alpha_\infty \rho_0}{\varphi}\left[1 + \frac{\sigma\varphi}{j\omega\rho_0\alpha_\infty}\sqrt{1 + j\frac{4\alpha_\infty^2 \eta \rho_0 \omega}{\sigma^2 \Lambda^2 \varphi^2}}\right] \tag{1}$$

The dynamic bulk modulus in the JCA model is given by

$$\widetilde{K}(\omega) = \frac{\gamma P_0/\varphi}{\gamma - (\gamma - 1)\ \left[1 - j\frac{8\kappa}{\Lambda'^2 C_p \rho_0 \omega}\sqrt{1 + j\frac{\Lambda'^2 C_p \rho_0 \omega}{16\kappa}}\right]^{-1}} \tag{2}$$

The variables in Eq. (1) and Eq. (2) are listed below:

- σ: the static air flow resistivity;
- φ: the open porosity;

- α_∞: the high frequency limit of the dynamic tortuosity;
- Λ: the viscous characteristic length;
- Λ': the thermal characteristic length

Moreover, there are some constant parameters displayed as follows:

- $\gamma = 1.4$: Heat capacity ratio,
- $\eta = 1.002\ \mathrm{mPa\cdot s}$: Dynamic (shear) viscosity
- $C_p = 1\mathrm{kJ/(kg*K)}$: Isobaric mass heat capacity,
- $\rho_0 = 1000\mathrm{g/m^2}$: air density
- $\kappa = 0.02\mathrm{W/(m*K)}$: thermal conductivity,

The characteristic impedance can be derived by Eq. (1) and Eq. (2) as follows:

$$Z_c = \sqrt{\tilde{\rho}(\omega)\tilde{K}(\omega)} \tag{3}$$

And the wave number:

$$k_c = \omega\sqrt{\frac{\tilde{\rho}(\omega)}{\tilde{K}(\omega)}} \tag{4}$$

The transfer matrix method [7] is adopted to calculate the surface impedance Z_s, then the absorption coefficient is obtained:

$$\alpha = 1 - [\frac{Z_s - \rho_0 c_0}{Z_s + \rho_0 c_0}]^2 \tag{5}$$

In the Section 4, the numerical results will be validated by comparing with the experimental results.

3. Samples

In order to validate our model, three kinds of plain weave samples are picked up which have different diameters of monofilaments and the monofilament spacing, and their normal incidence absorption coefficients are measured by impedance tube. All of three types of samples are made in nylon monofilament, in other words, there is no intrayarn air flow in our samples.

The parameters of three kinds of sample are shown in Table 1:

Table 1: The parameters of material used in experimental method

	diameter of monofilament(μm)	monofilament spacing(μm)
Sample1	35	35
Sample2	28	50
Sample3	48	100

According to the three types of samples mentioned above, the parameters are contained which we need in the JCA model by using FEM method, which are listed in the Table 2. Moreover, the data of optimal flow resistivity of every case is calculated according to the formula in Pieren [1].

Table 2: The parameters of 3D model

	case	φ	Λ (mm)	Λ' (mm)	α_∞	σ (Ns/m^4)	$\sigma_{s,opt}$ (Ns/m^4)
Sample1	$h_j = 0$	0.70	0.015	0.03	1.3	765000	1600000
	$h_j = h_w$	0.55	0.01	0.02	1.4	164000	3300000
Sample2	$h_j = 0$	0.76	0.03	0.07	1.2	230000	1660000
	$h_j = h_w$	0.65	0.02	0.03	1.3	419000	3420000
Sample3	$h_j = 0$	0.82	0.06	0.11	1.15	56000	740000
	$h_j = h_w$	0.74	0.05	0.07	1.2	95000	1560000

4. Comparison and discussion

Normal incidence absorption coefficients of three samples are measured by a Brüel & Kjaer two-microphone impedance tube of type 4206, according to the standard ISO (10534-2). The frequency range of measures is from 0 to 1600 Hz.

The comparisons between the numerical and experimental results are represented in Fig. 4 to Fig. 6.

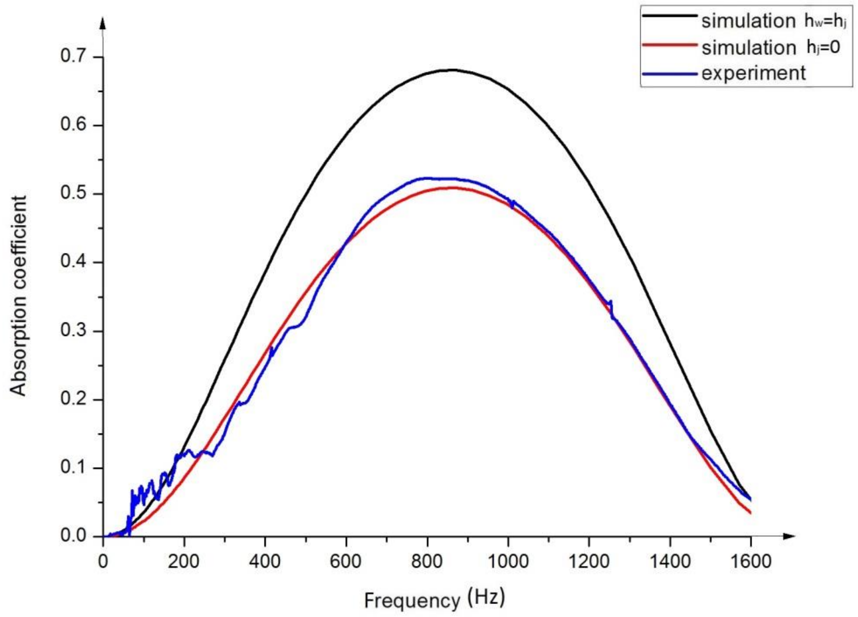

Figure 4: Sample 1 with the depth of air cavity D=0.1m

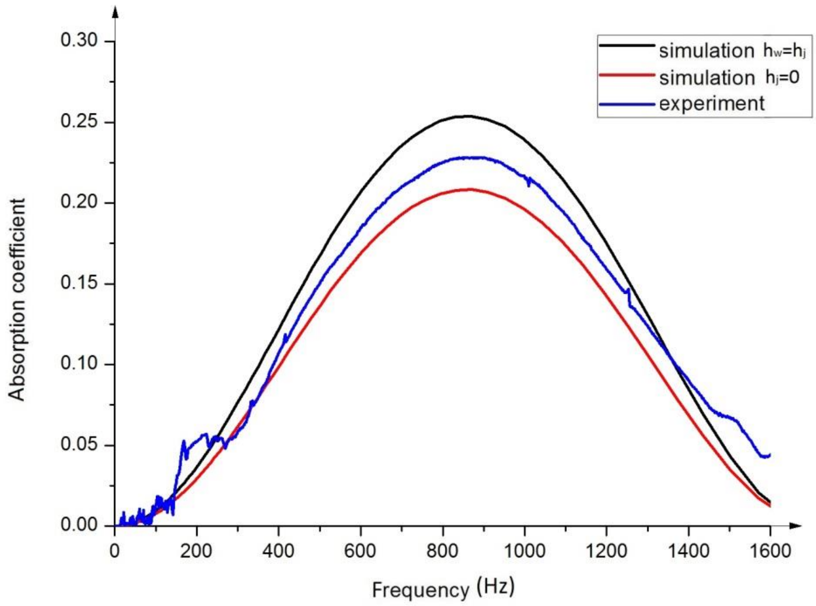

Figure 5: Sample 2 with the depth of air cavity D=0.1m

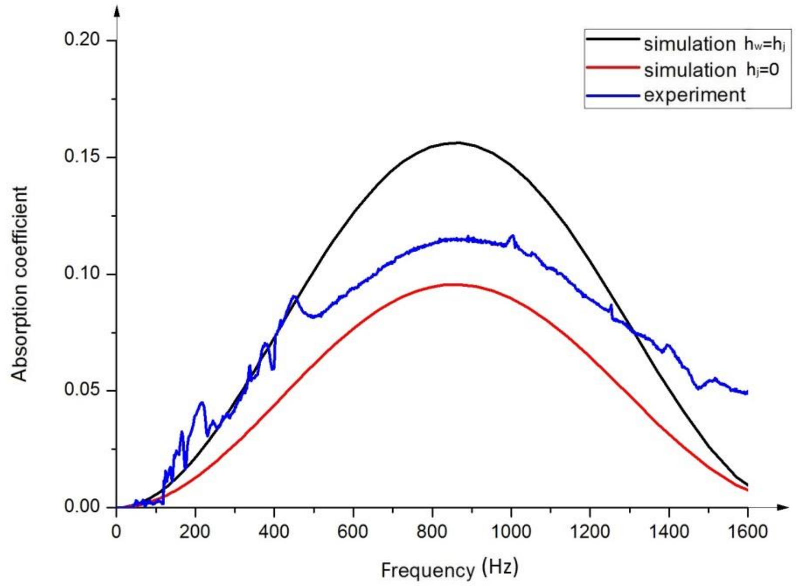

Figure 6: Sample 3 with the depth of air cavity D=0.1m

In Fig. 4 to Fig. 6, the results of impedance tube experiments are between the two extreme cases. The details of the relationship between h_j and h_w in the samples depend on the microstructure.

However, the performance of the case $h_j = h_w$ in sound absorption is better than the case $h_j = 0$ in all kinds of samples. In the results of sample 1, the peak value of $h_j = h_w$ is over 0.6, though it is just 0.5 in the case of $h_j = 0$. It is mainly because the data of porosity and flow resistivity of two cases are different. The same tendency in all of three samples is observable in the Table 2 that the case $h_j = h_w$ has the smaller porosity and greater flow resistivity than the case $h_j = 0$. Besides, the data of flow resistivity of three samples are much smaller than the optimal specific airflow. Moreover, when the data of the two characteristic lengths and the dynamic tortuosity are changed in reasonable ranges, the changes of the absorption coefficients are negligible. Therefore, the sound absorption is more significantly influenced by the porosity and the flow resistivity than other parameters.

5. Conclusion

The JCA model is used to obtain the absorption coefficients of plain weave, and the numerical results are validated by comparison with the experimental results. Meanwhile, the results represent that the sound absorption is strongly influenced by the crimp height. It means that the weaving machine should be improved to make the warp and weft crimp height more close to each other. Moreover, according to the numerical results, the sound absorption is more significantly influenced by the porosity and the flow resistivity than other parameters. By improving the weaving machine and choosing appropriate diameter of monofilament, an acoustic textile can be fabricated for the engineering application.

Acknowledgment

This work has been supported by the National Natural Science Foundation of China under Grant No. 11604015 and 11274048, Beijing Natural Science Foundation No.8142016 and 1172007, Innovation Team IG201501C2, Xicheng Excellent Talents Project No.20150057 and Youth Backbone 201502.

REFERENCES

1 Pieren, R. Sound absorption modeling of thin woven fabrics backed by an air cavity, *Textile Research Journal*, **82**(9), 864-874, (2012),.

2 Pieren, R., Heutschi, K. Predicting sound absorption coefficients of lightweight multilayer curtains using the equivalent circuit method, *Applied Acoustics*, **92**, 27-41, (2015).

3 Ruiz, H., Cobo, P., Jacobsen F. Optimization of multiple-layer microperforated panels by simulated annealing, *Applied Acoustics*, **72**(10), 772-776, (2011).

4 F. T. Peirce D.Sc., F. Inst. P. and F. T. I. The geometry of cloth structure, *Journal of the Textile Institute Transactions*, **28**(3),T45-T96, (1937).

5 Johnson, D. L., Koplik, J. and Dashen, R., Theory of dynamic permeability and tortuosity in fluid-saturated porous media, *Journal of Fluid Mechanics*, **176**(176), 379-402, (1987).

6 Champoux, Y., Allard, J. F., Dynamic tortuosity and bulk modulus in air-saturated porous media, *Journal of Applied Physics*, **70**(4), 1975-1979, (1991).

7 Allard, J. F., Atalla, N., Propagation of sound in porous media: modelling sound absorbing materials, John Wiley & Sons, (2009).